Science Advances
AAAS

Manuscript Template

FRONT MATTER

Title

Bio-inspired jellyfish microparticles from microfluidics for water decontamination

Authors

Chaoyu Yang[1,2,] Yunru Yu[1,2], Luoran Shang[3,*], Yuanjin Zhao[1,2,4*]

Affiliations

1. Department of Clinical Laboratory, The Affiliated Drum Tower Hospital of Nanjing University Medical School, 210008 Nanjing, China

   E-mail: yjzhao@seu.edu.cn

2. Oujiang Laboratory (Zhejiang Lab for Regenerative Medicine, Vision and Brain Health), Wenzhou Institute, University of Chinese Academy of Sciences, Wenzhou, Zhejiang 325001, China

3. Shanghai Xuhui Central Hospital, Zhongshan-Xuhui Hospital, and the Shanghai Key Laboratory of Medical Epigenetics, the International Co-laboratory of Medical Epigenetics and Metabolism (Ministry of Science and Technology), Institutes of Biomedical Sciences, Fudan University, Shanghai, China.

   E-mail: luoranshang@fudan.edu.cn

4. State Key Laboratory of Bioelectronics, School of Biological Science and Medical Engineering, Southeast University, Nanjing 210096, China

Abstract

Water decontamination is vital for both environmental protection and human health. Particle-based adsorbents are excellent candidates for water purification owing to their high specific surface area and adsorption efficiency. To further improve the adsorption performance, those particles are expected to possess tailored structures and flexible motion ability. Herein, inspired by the free-swimming jellyfish, we present jellyfish-shaped microparticles via microfluidics for adsorbing water impurities. By introducing piezoelectric pulse vibrations to a jet flow, jellyfish particles with finely tunable size and morphologies can be continuously generated. Attractively, by employing stimuli-responsive composite hydrogel along with magnetic nanoparticles, the resultant particles show dual-stimuli-triggered movement ability under combinational control. These unique features contributed to enhanced adsorption efficiency due to the increased change of contact between the particles and the impurities. This study not only demonstrates the superiority of the jellyfish particles for water decontamination, but also inspires microfluidic fabrication of anisotropic particles for various use.

One-Sentence Summary: Inspired by jellyfish, a novel particle adsorbent is developed using piezoelectric microfluidics for water decontamination.

MAIN TEXT

Introduction

The impurity in water is one of the major problems of the whole world that keeps challenging environmental protection and human health **(*1-4*)**. With increasing attention to these aspects, various adsorbent materials have been developed to remove different impurities from water, such as adsorption column, scaffold, film, and so on **(*5-10*)**. However, most of the currently available adsorbents are bulk materials with a small specific surface area, which limits the contact surfaces and restricts the adsorption efficiency **(*11-13*)**. As an alternative, the emerging particle-based materials are playing significant roles in highly efficient adsorption **(*14-16*)**. These functional particles, obtained via chemical synthesis, emulsion templates, and others, have demonstrated values in the removal of oils, impurities, heavy metals, organic solvents, and so on **(*11, 14-18*)**. Although with many successes, the existing particle adsorbents are often with simple geometries while their shape anisotropy has not been fully explored, which limited their flexibility in adsorption. In addition, the uncontrollable motion of these particles in water also obstacles their active and efficient adsorption of impurities. Thus, an intelligent adsorbent with designed architecture and flexible controllability is still anticipated.

Here, inspired by the morphology and locomotion of jellyfish, we presented novel particles with jellyfish-like structures and controllable movement capabilities by using microfluidics for water decontamination, as schemed in **Figure 1A**. With the advantages in precise control of fluids in constrained channels, microfluidics has emerged as a promising method for the generation of various particles **(*19-23*)**. However, due to the restriction of channel geometry and interfacial tension on the droplet templates, the resultant particles are generally spherical or slightly deviated from spherical **(*16, 24-31*)**, while highly anisotropic particle shapes are still difficult to achieve. By contrast, jellyfish is a class of free-swimming marine coelenterate with an umbrella-shaped body **(*32, 33*)**. Such a unique shape facilitates the motion of jellyfishes by radially expanding/contracting their body and thus pushing water behind **(*34, 35*)**. The flexible swimming ability also helps jellyfishes enhance the contact with the potential prey targets **(*36*)**. It is thus conceived that, by using microfluidics to construct jellyfish-like particles with flexible and controllable motion ability, smart and efficient adsorption of water contaminants could be realized.

In this paper, we employed a pulse-generating microfluidic system to generate bio-inspired microparticles with jellyfish-like structures for smart adsorption and water purification. By combining piezoelectric vibration with co-flow microfluidics, a fluid thread with periodic re-entrance cavities was generated, which then evolved to form jellyfish-like droplets and eventually particles. By adjusting the piezoelectric parameters, the morphology of the resultant particles could be easily controlled. Besides, by incorporating graphene oxide/N-Isopropylacrylamide (GO/NIPAM), the microparticles exhibited stimuli-responsive shrinkage behavior under near-infrared (NIR) irradiation. Owing to the anisotropic particle shape, such deformation could provide a propulsive thrust to propel the particle, in a way mimicking the jellyfish (**Figure 1B**). Besides, by further incorporating magnetic nanoparticles (NPs), the direction of movement of the particles could be controlled by a magnet. These features facilitated flexible motion of the particles in water and thus enhanced the contact with water contaminants. Based on that, we demonstrated the capability of the jellyfish-like microparticles in highly efficient adsorption of organic pollutants under external control (**Figure 1B**). These resultants indicated the superiority of

the jellyfish-shaped particles in active motion and water decontamination, and extended the availability of microfluidics in constructing functional materials.

Results

In a typical experiment, we assembled a co-flow microfluidic device by coaxially inserting a tapered injection capillary into an outer collection capillary (**Figure S1**). An inner aqueous pre-gel solution (PEG-diacrylate, PEGDA) and the outer fluid of deionized water were simultaneously driven to the injection and collection capillary, respectively, and flowed in the same direction to form a steady jet formed downstream in the collection capillary. A piezoelectric stack was employed to exert oscillation pulsations to the inner phase, and the inner phase fluid was modulated as desired. When the amplitude of pulsation exceeded a certain value, the fluctuation caused the inner jet to periodically retract and go forward, and then formed droplets with a varicose head and thin-thread tail (**Figure 2A**). Due to the large inertial force relative to the interfacial tension of the two aqueous phases **(*37*)**, the droplets continued to deform into a jellyfish-like shape in accordance with Poiseuille advection (**Movie S1**). Then the effects of the piezoelectric parameters on the jellyfish droplet were systematically investigated in detail (**Figure 2B**, **2C**). It was found that the length *l* and head ratio *h/l* could be well controlled by respectively changing the piezoelectric frequency and voltage, as plotted in **Figure 2D**, **2E**. These results demonstrated that by simply programming the piezoelectric signals, the jellyfish-like droplet templates with controllable morphologies could be obtained on demand.

After rapid solidification by UV irradiation, the jellyfish-like droplet templates were polymerized into solid particles with the same shape. The resultant particles possessed an umbrella-like head with an internal cavity and a trailing tentacle and showed component homogeneity (**Figure 3A)**. The morphology was further confirmed by scanning electron microscopy (SEM), as depicted in **Figure 3B**. Since the morphology of the droplet templates evolved from bullet to jellyfish at the microfluidic channel, by shinning UV at different positions of the collection tube, the resultant particles could preserve the corresponding morphologies (**Figure S2**). Benefiting from the continuous fluid flow in microfluidics, this method enabled consecutive generation of jellyfish-like particles with uniform size and morphology, as shown in **FiguRE 3C**, **3D**. Moreover, the jellyfish particle length could be finely tuned by altering the piezoelectric frequency, as shown in **Figure 3E**. The length distribution of the jellyfish particles demonstrated the monodispersity, with a coefficient of variation <5% (the SD divided by the mean value), as plotted in **Figure 3F**.

Intriguingly, by taking advantage of the flexibility in fluidic manipulation of microfluidics, we prepared dual-layered jellyfish-like microparticles. Specifically, a capillary microfluidic device was constructed comprising a two-stage nested channel design (**Figure S3**), and the piezoelectric vibration was induced to the middle phase (**Figure 4A**). The two inner fluids were pumped to the microfluidic channel and pulsed periodically, forming a dual-layered stream, which eventually resulted in the formation of dual-layered jellyfish-like microparticles (**Figure 4B**). We demonstrated the dual-layered structure of the particles in both the head and the tail through CLSM (**Figure 4C, Movie S2**). Besides, by tuning the microfluidic parameters (the innermost phase flow rate Q_i and the middle phase flow rate Q_m), the proportion of the two components could be controlled by $\varphi = Q_i/(Q_i+Q_m)$, as shown in **Figure S4**. When Q_i+Q_m was fixed, the increase of φ would result in the increase of the inner layer thickness, as plotted in **Figure 4D**. Similar to that of the simple jellyfish microparticles, the dual-layered jellyfish-like particles could also be continuously fabricated with uniform size and morphology, as shown in **Figure 4E**. Such dual-layered structure of the particles could facilitate the addition of functional ingredients as needed, thus supporting various functionalities.

To impart the particles with stimuli-triggered motion ability, functional GO/NIPAM composite hydrogels were employed as the component of the dual-layered particles so that they could respond to NIR. Benefiting from the photo-thermal effect of the GO/NIPAM hydrogel, the particles could undergo contraction under NIR irradiation. As a result, the particles could be propelled to move forward. We validated this process by tracking the displacement of a single particle under NIR irradiation, as shown in **Figure 5A, 5B** and **Movie S3**. Besides, by incorporating Fe_3O_4 NPs to the innermost layer, the particles could be endowed with additional magneto-responsiveness. As the Fe_3O_4 NPs were dispersed in the inner layer of the particles and occupied a large proportion in the head, the response of the particles to the magnetic field should be asymmetric, thus facilitating controllable movement. When the particles were placed in a relatively weak field, they re-orientated and turned their heads toward the magnet (**Figure 5C, 5D** and **Movie S4)**. When the magnetic field was further enhanced, the particles would move directionally to the magnet side, as shown in **Figure 5E, 5F** and **Movie S5**. These features demonstrated the prominent controllability of the bio-inspired jellyfish-like microparticles under multiple external stimuli.

Due to the versatile motion controllability features, the multi-stimuli-responsive jellyfish particles were expected to be applied in the adsorption of water impurities. Besides, since GO owns extraordinarily large surface areas and large numbers of polar groups, it has a natural advantage in impurity adsorption ***(38, 39)***. We tested the adsorption of a model dye, methylene blue (MB), using these microparticles under combinational control of magnetic field and NIR (**Figure 6**). The particles could be drawn from one side of the cuvette to the other by alternating the direction of the magnet (**Figure S5**). Besides, NIR irradiation could be exerted to cause a circulation of the swarm of particles and thus enhancing the contact of the particles with the dyes in the solution (**Figure 6B**). Benefiting from these effects, the particles under dual stimuli achieved the best adsorption performance, as manifested by the color change (**Figure 6A**). It was also found that with sufficient adsorption, the color of the particles changed from brown to blue, indicating that the pollutants were adsorbed by these particles, as shown in **Figure 6C**, **6D**. Then we studied the adsorption kinetics of these particles with different stimulation modes. We measured the real-time concentration of MB (C) relative to its initial concentration (C_0) at different time points for each group, as plotted in **Figure 6E**. It was found that the magnetic-stimuli group showed faster and more effective adsorption capability than the non-stimuli group due to efficient movement. In addition, the magnet/NIR-stimuli group showed superior adsorption capability even to the magnetic-stimuli group, which suggested that the particles under combinational control could have a larger chance of contact with the pollutants in the solution.

Discussion

In summary, we have developed novel bio-inspired jellyfish microparticles with smart adsorption capacities from microfluidics for water decontamination. The jellyfish microparticles were derived from droplet templates through piezoelectric pulsation of a fluid jet. The size and morphology of the particles were readily overmastered by altering the piezoelectric frequency and voltage. Besides, multi-compartment jellyfish microparticles with dual-layer structures were facilely achieved by tailoring the channel geometry of the microfluidics. Moreover, by employing GO/NIPAM hydrogel precursor and magnetic nanoparticles into the droplet templates, the resultant jellyfish microparticles were imparted with dual-stimuli responsiveness, i.e., NIR and magnetic field. This allowed

for the versatile motion of the particles including re-orientation and directional movement. Such distinct characteristics of the bio-inspired particles enhanced their adsorbing efficiency, making them excellent adsorbents for water decontamination and promising materials for other related areas including biomimetics, smart robotics, etc. We believe this study would also shed light on the microfluidic fabrication of anisotropic microparticles that would open an avenue to a wide range of applications.

Materials and Methods

Materials

PEG-diacrylate (PEGDA, average Mn = 700), *N*, *N*′-methylenebis (acrylamide) (BIS) and photoinitiator 2-hydroxy-2-methylphenylpropanone (HMPP) were all procured from Sigma-Aldrich. Fluorescent polystyrene (PS) nanoparticles (F8805 and F8811) were procured from Invitrogen. Graphene oxide (GO) solution (2 mg/mL) was bought from XF NANO Co., Ltd. N-Isopropylacrylamide (NIPAM, 97%) and Methylene Blue (MB) were bought from Macklin. Photo-initiator Lithium phenyl(2,4,6-trimethylbenzoyl) phosphinate (LAP) was derived from Aladdin. Magnetic nanoparticles were synthesized by a hydrothermal method.

Piezoelectric Microfluidics Construction

The microfluidics was constructed by coaxially aligning two capillaries on a glass slide. The inner circular capillary (capillary 2), with an inner and outer diameter of 580 μm and 1.0 mm (World Precision Instruments), was tapered by a capillary puller (Sutter Instrument, P-97) and then sanded to the desired diameter (200 μm) by a microforge (Narishige, MF-830). The outer capillary (capillary 3) was also a cylindrical capillary (inner diameter: 1560 μm, outer diameter: 2 mm). Capillary 2 served as the injection tube and capillary 3 was used as the collection tube. For the generation of dual-layered particles, another capillary (capillary 1) with an orifice diameter of about 150 μm was coaxially inserted into capillary 2, and these two capillaries were coaxially aligned in capillary 3 to form a two-stage nested configuration. Capillary 1 and capillary 2 served as the innermost and middle injection channels and capillary 3 served as the outer fluid channel. The joints of these capillaries were sealed by transparent epoxy resin where necessary. To generate jellyfish droplet templates, a piezoelectric stack was employed to transmit the sinusoidal signal to the corresponding fluid. The piezoelectric stack actuator was connected to a signal generator (Siglent, SDG 2000X) via a power amplifier (Core morrow, E-05) to program the amplitudes and frequencies. In this paper, the magnification of the power amplifier was fixed as 12x, and the voltages mentioned throughout the manuscript were in the form of $V_{p\text{-}p}$ (peak-to-peak) of the signal generator.

Jellyfish particles generation

For the generation of single-layer jellyfish particles, the inner phase was an aqueous solution of PEGDA (15% v/v) with photoinitiator HMPP (1% v/v) and the outer phase was deionized water. Both solutions were driven into the corresponding channels by two syringe pumps (Longer, LSP01-2A) and the inner phase was connected to the piezoelectric stack actuator. For observing the dynamics of the generation of the droplet template, the flow rates were Q_i = 5 mL/h and Q_o = 70 mL/h. For the generation of simple jellyfish particles, the typical set of the flow rates was Q_i = 5 mL/h and Q_o = 55 mL/h, respectively. For the generation of

the dual-layered jellyfish particles, the innermost phase and the middle phase were both aqueous solutions of PEGDA (15% v/v) with HMPP (1% v/v), and the outer phase was deionized water. Red and green fluorescent polystyrene (PS) nanoparticles were added to the innermost and middle phases, respectively (each with a concentration of 0.5% v/v), for CLSM imaging. These solutions were all pumped to the corresponding channels, and the middle phase was actuated by the piezoelectric stack actuator. A typical set of the flow rates was Q_i = 1.5 mL/h, Q_m= 3.5 mL/h,and Q_o = 55 mL/h. For the generation of multi-stimuli-responsive particles, the innermost phase was a mixture solution of GO (1 mg/mL), NIPAM (4% v/v), PEGDA (8% v/v), BIS (corresponding to 1/30 to the mass of NIPAM), and LAP (0.1% v/v); the middle phase was a mixture solution of GO (2 mg/mL), NIPAM (8% v/v), PEGDA (8% v/v), BIS (corresponding to 1/30 to the mass of NIPAM), and LAP (0.1% v/v); the outer phase was deionized water. The flow rates were Q_i = 1.5 mL/h, Q_m = 3.5 mL/h, and Q_o = 55 mL/h. In all cases, the jellyfish-like droplet templates were rapidly solidified downstream upon *in-situ* ultraviolet (UV) irradiation with double heads (EXFO OmniCure SERIES 1000, 365nm, 100W).

Characterization

The jellyfish template generation dynamics was recorded by a microscope equipped with a fast camera (AcutEye). The optical and fluorescence microscopic images of the bio-inspired particles were captured by a fluorescent microscope (OLYMPUS, CKX53) with a CCD. Cross-section fluorescence images of the particles were taken by a Laser Scanning Confocal Microscope (LSCM, Leica, STELLARIS). The microstructures of the solidified jellyfish microparticle were captured by scanning electron microscopy (SEM, HITACHI, SU8010).

Studying the adsorption kinetics of the bio-inspired particles

Methylene blue (MB) was used as the model pollutant to test the adsorption performance of the resultant bio-inspired particles. The adsorption experiments were performed at room temperature (25 ℃). The MB concentration in water was obtained at 662 nm by a microplate reader (Epoch, BIO-TEK). The number of replicates was 3. For the magnetic stimuli, the direction of the magnetic field was alternated every 5 min to pull the jellyfish microparticles from one side of the container to the other side. For NIR stimuli, after changing the magnet direction, the particles were exposed to laser (808 nm) irradiation for 1 min every 5 mins at a distance of 10 cm.

H2: Supplementary Materials

Figure S1. Microfluidic chip for simple jellyfish particles.
Figure S2. Morphologies of bio-inspired particles at different irradiation positions.
Figure S3. Microfluidic chip with two-stage nested channels for dual-layered jellyfish particles.
Figure S4. Composition control with flow rates.
Figure S5. Magnet control on the adsorption process.

Movie S1. Dynamics of jellyfish droplet template in the microfluidics.
Movie S2. CLSM 3D reconstruction of the dual-layered jellyfish particle.
Movie S3. Movement of a single dual-layered jellyfish particle under NIR irradiation.
Movie S4. Re-orientation of the magnetic-responsive dual-layered jellyfish microparticles under a weak magnetic field.
Movie S5. Directional migration of the magnetic-responsive dual-layered jellyfish microparticles under a strong magnetic field.

References

1. M. MacLeod, H. P. H. Arp, M. B. Tekman, A. Jahnke, The global threat from plastic pollution. *Science* **373**, 61-65 (2021).
2. D. M. Mitrano, P. Wick, B. Nowack, Placing nanoplastics in the context of global plastic pollution. *Nat. Nanotechnol.* **16**, 491-500 (2021).
3. C. Yu, X. Huang, H. Chen, H. C. J. Godfray, J. S. Wright, J. W. Hall, P. Gong, S. Ni, S. Qiao, G. Huang, Managing nitrogen to restore water quality in China. *Nature* **567**, 516-520 (2019).
4. M. Zou, Y. Zhang, Z. Cai, C. Li, Z. Sun, C. Yu, Z. Dong, L. Wu, Y. Song, 3D Printing a Biomimetic Bridge - Arch Solar Evaporator for Eliminating Salt Accumulation with Desalination and Agricultural Applications. *Adv. Mater.* **33**, 2102443 (2021).
5. R. Ou, H. Zhang, V. X. Truong, L. Zhang, H. M. Hegab, L. Han, J. Hou, X. Zhang, A. Deletic, L. Jiang, A sunlight-responsive metal–organic framework system for sustainable water desalination. *Nat. Sustain.* **3**, 1052-1058 (2020).
6. L. Yang, H. Xiao, Y. Qian, X. Zhao, X.-Y. Kong, P. Liu, W. Xin, L. Fu, L. Jiang, L. Wen, Bioinspired hierarchical porous membrane for efficient uranium extraction from seawater. *Nat. Sustain.*, 1-10 (2021).
7. M. Peydayesh, M. K. Suter, S. Bolisetty, S. Boulos, S. Handschin, L. Nyström, R. Mezzenga, Amyloid fibrils aerogel for sustainable removal of organic contaminants from water. *Adv. Mater.* **32**, 1907932 (2020).
8. Y. Guo, X. Zhou, F. Zhao, J. Bae, B. Rosenberger, G. Yu, Synergistic energy nanoconfinement and water activation in hydrogels for efficient solar water desalination. *ACS nano* **13**, 7913-7919 (2019).
9. S. Xie, S. Wu, S. Bao, Y. Wang, Y. Zheng, D. Deng, L. Huang, L. Zhang, M. Lee, Z. Huang, Intelligent mesoporous materials for selective adsorption and mechanical release of organic pollutants from water. *Adv. Mater.* **30**, 1800683 (2018).
10. A. L. Taka, M. J. Klink, X. Y. Mbianda, E. B. Naidoo, Chitosan nanocomposites for water treatment by fixed-bed continuous flow column adsorption: a review. *Carbohydr. Polym.* **255**, 117398 (2021).
11. D. Weng, L. Song, W. Li, J. Yan, L. Chen, Y. Liu, Review on synthesis of three-dimensional graphene skeletons and their absorption performance for oily wastewater. *Environ. Sci. Pollut. Res.* **28**, 16-34 (2021).
12. Y. Chen, L. Chen, H. Bai, L. Li, Graphene oxide–chitosan composite hydrogels as broad-spectrum adsorbents for water purification. *J. Mater. Chem. A* **1**, 1992-2001 (2013).
13. O. Halevi, T.-Y. Chen, P. S. Lee, S. Magdassi, J. A. Hriljac, Nuclear wastewater decontamination by 3D-Printed hierarchical zeolite monoliths. *RSC Adv.* **10**, 5766-5776 (2020).
14. L. Sun, J. Wang, Y. Yu, F. Bian, M. Zou, Y. Zhao, Graphene oxide hydrogel particles from microfluidics for oil decontamination. *J. Colloid Interface Sci.* **528**, 372-378 (2018).
15. X. Deng, Y. Ren, L. Hou, T. Jiang, H. Jiang, Continuous microfluidic fabrication of anisotropic microparticles for enhanced wastewater purification. *Lab Chip* **21**, 1517-1526 (2021).
16. M. Ren, W. Guo, H. Guo, X. Ren, Microfluidic fabrication of bubble-propelled micromotors for wastewater treatment. *ACS Appl. Mater. Interfaces* **11**, 22761-22767 (2019).
17. J. H. Pan, X. Zhang, A. J. Du, D. D. Sun, J. O. Leckie, Self-etching reconstruction of hierarchically mesoporous F-TiO2 hollow microspherical photocatalyst for concurrent membrane water purifications. *J. Am. Chem. Soc.* **130**, 11256-11257 (2008).
18. B. Jurado-Sánchez, J. Wang, Micromotors for environmental applications: a review. *Environmental Science: Nano* **5**, 1530-1544 (2018).

19. Y. Yu, L. Shang, J. Guo, J. Wang, Y. Zhao, Design of capillary microfluidics for spinning cell-laden microfibers. *Nat. Protoc.* **13**, 2557-2579 (2018).
20. C. Yang, Y. Yu, X. Wang, L. Shang, Y. Zhao, Programmable Knot Microfibers from Piezoelectric Microfluidics. *Small*, 2104309 (2021).
21. Q. Wu, C. Yang, G. Liu, W. Xu, Z. Zhu, T. Si, R. X. Xu, Multiplex coaxial flow focusing for producing multicompartment Janus microcapsules with tunable material compositions and structural characteristics. *Lab Chip* **17**, 3168-3175 (2017).
22. Y. Cheng, C. Zhu, Z. Xie, H. Gu, T. Tian, Y. Zhao, Z. Gu, Anisotropic colloidal crystal particles from microfluidics. *J. Colloid Interface Sci.* **421**, 64-70 (2014).
23. Y. Wang, X. Zhang, L. Shang, Y. Zhao, Thriving microfluidic technology. *Sci. Bull.* **66**, 9-12 (2021).
24. M. Hua, Y. Du, J. Song, M. Sun, X. He, Surfactant-free fabrication of pNIPAAm microgels in microfluidic devices. *J. Mater. Res.* **34**, 206-213 (2019).
25. L. Cai, F. Bian, H. Chen, J. Guo, Y. Wang, Y. Zhao, Anisotropic microparticles from microfluidics. *Chem* **7**, 93-136 (2021).
26. C. Yang, R. Qiao, K. Mu, Z. Zhu, R. X. Xu, T. Si, Manipulation of jet breakup length and droplet size in axisymmetric flow focusing upon actuation. *Phys. Fluids* **31**, 091702 (2019).
27. L. Cai, G. Chen, Y. Wang, C. Zhao, L. Shang, Y. Zhao, Boston ivy-inspired disc-like adhesive microparticles for drug delivery. *Research* **2021**, (2021).
28. M.-Y. Zhang, K. Xu, J.-H. Xu, G.-S. Luo, Self-assembly kinetics of colloidal particles inside monodispersed micro-droplet and fabrication of anisotropic photonic crystal micro-particles. *Crystals* **6**, 122 (2016).
29. C. Zhou, P. Zhu, Y. Tian, M. Xu, L. Wang, Engineering micromotors with droplet microfluidics. *ACS nano* **13**, 6319-6329 (2019).
30. T. Nisisako, T. Ando, T. Hatsuzawa, Capillary - Assisted Fabrication of Biconcave Polymeric Microlenses from Microfluidic Ternary Emulsion Droplets. *Small* **10**, 5116-5125 (2014).
31. K. Xu, J.-h. Xu, Y.-c. Lu, G.-S. Luo, A novel method of fabricating, adjusting, and optimizing polystyrene colloidal crystal nonspherical microparticles from gas–water janus droplets in a double coaxial microfluidic device. *Cryst. Growth Des.* **14**, 401-405 (2014).
32. N. W. Xu, J. O. Dabiri, Low-power microelectronics embedded in live jellyfish enhance propulsion. *Sci. Adv.* **6**, eaaz3194 (2020).
33. Z. Ren, W. Hu, X. Dong, M. Sitti, Multi-functional soft-bodied jellyfish-like swimming. *Nat. Commun.* **10**, 1-12 (2019).
34. A. P. Hoover, N. W. Xu, B. J. Gemmell, S. P. Colin, J. H. Costello, J. O. Dabiri, L. A. Miller, Neuromechanical wave resonance in jellyfish swimming. *Proc. Natl. Acad. Sci.* **118**, (2021).
35. J. H. Costello, S. P. Colin, J. O. Dabiri, B. J. Gemmell, K. N. Lucas, K. R. Sutherland, The hydrodynamics of jellyfish swimming. *Annu. Rev. Mar. Sci.* **13**, 375-396 (2021).
36. M. Dawoodian, A. Sau, Kinetics and prey capture by a paddling jellyfish: three-dimensional simulation and Lagrangian coherent structure analysis. *J. Fluid Mech.* **912**, (2021).
37. A. Sauret, C. Spandagos, H. C. Shum, Fluctuation-induced dynamics of multiphase liquid jets with ultra-low interfacial tension. *Lab Chip* **12**, 3380-3386 (2012).
38. S. Chowdhury, R. Balasubramanian, Recent advances in the use of graphene-family nanoadsorbents for removal of toxic pollutants from wastewater. *Adv. Colloid Interface Sci.* **204**, 35-56 (2014).
39. J. C. Meyer, A. K. Geim, M. I. Katsnelson, K. S. Novoselov, T. J. Booth, S. Roth, The structure of suspended graphene sheets. *Nature* **446**, 60-63 (2007).

Acknowledgments

Funding: This work was supported by the National Key Research and Development Program of China (2020YFA0908200), the National Natural Science Foundation of China (22002018, 52073060 and 61927805), the Open Foundation of the State Key Laboratory of Molecular Engineering of Polymers (K2021-08), and the Shenzhen Fundamental Research Program (JCYJ20190813152616459).

Author contributions: Y. Z. conceived the idea and designed the experiment; C. Y. carried out the experiments and analyzed data; C. Y. and L. S. wrote the paper; Y. Y contributed to the scientific discussion of the article.

Competing interests: The authors declare no competing interests.

Figures

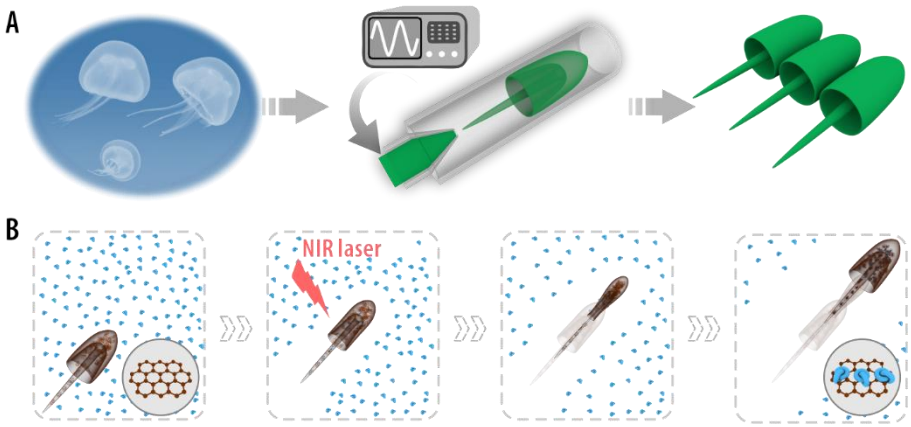

Fig. 1. Schematic illustrations of the generation and adsorption process of the jellyfish particles. (A) Schematic diagram of jellyfish, the piezoelectric microfluidic setup, and the bio-inspired jellyfish microparticles; **(B)** schematic diagram of the movement of a stimuli-responsive microparticle under NIR laser irradiation and the adsorption process for water contaminants.

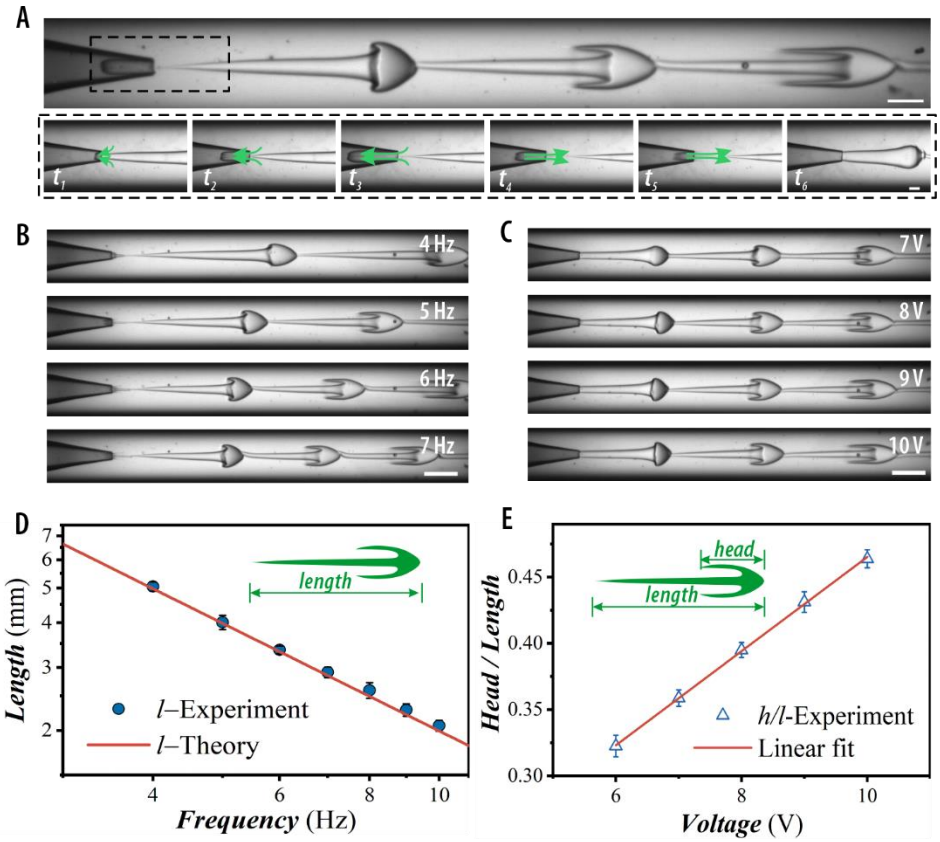

Fig. 2. Generation dynamics and morphology control of the jellyfish droplet template in microfluidics. (A) High-speed real-time images of the generation of jellyfish droplet template in the microfluidic collection tube. The bottom panels show an entire process of fluid retraction and advancement; **(B, C)** high-speed real-time images of the dynamic behaviors of the jellyfish droplet template under different (B) piezoelectric frequencies and (C) actuation amplitudes; **(D)** plot of the length of the jellyfish-like droplet template as a function of the piezoelectric frequency; **(E)** plot of the ratio of head to the length of the droplet template as a function of the piezoelectric voltage amplitude at the position of the third jellyfish in (C). The scale bars are 500 μm in the upper panel of (A), 250 μm in the bottom panels of (A), and 1000 μm in (B,C).

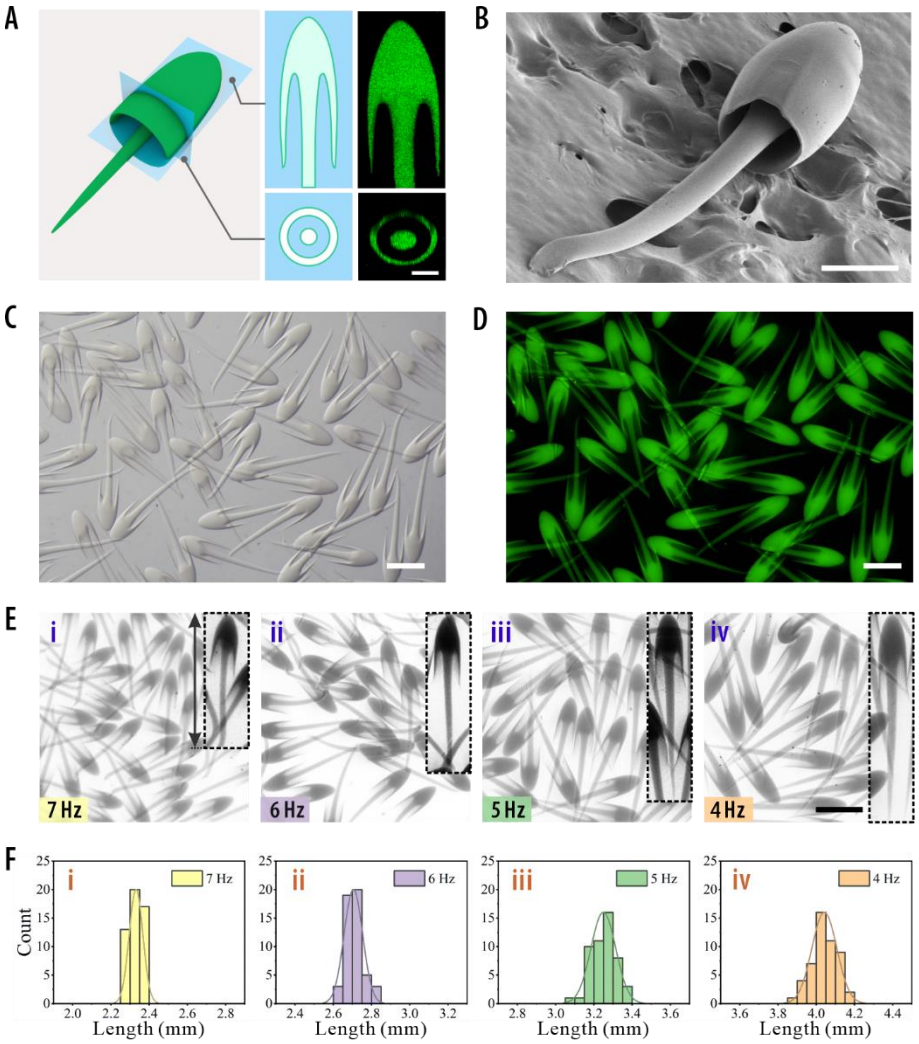

Fig. 3. Microfluidic and piezoelectric parameters on the jet template. (A) Schematic illustrations and cross-sectional confocal laser scanning microscope (CLSM) images of the resultant particle; **(B)** SEM image of one jellyfish particle; **(C, D)** microscopy images of a batch of bio-inspired particles with fluorescent polystyrene nanoparticles (C) in bright field and (D) fluorescent field; **(E)** jellyfish microparticles produced under different piezoelectric frequency; **(F)** the corresponding length distributions of the particles. The scale bars are 100 μm in (A), 200 μm in (B) and 1000 μm in (C, D, E).

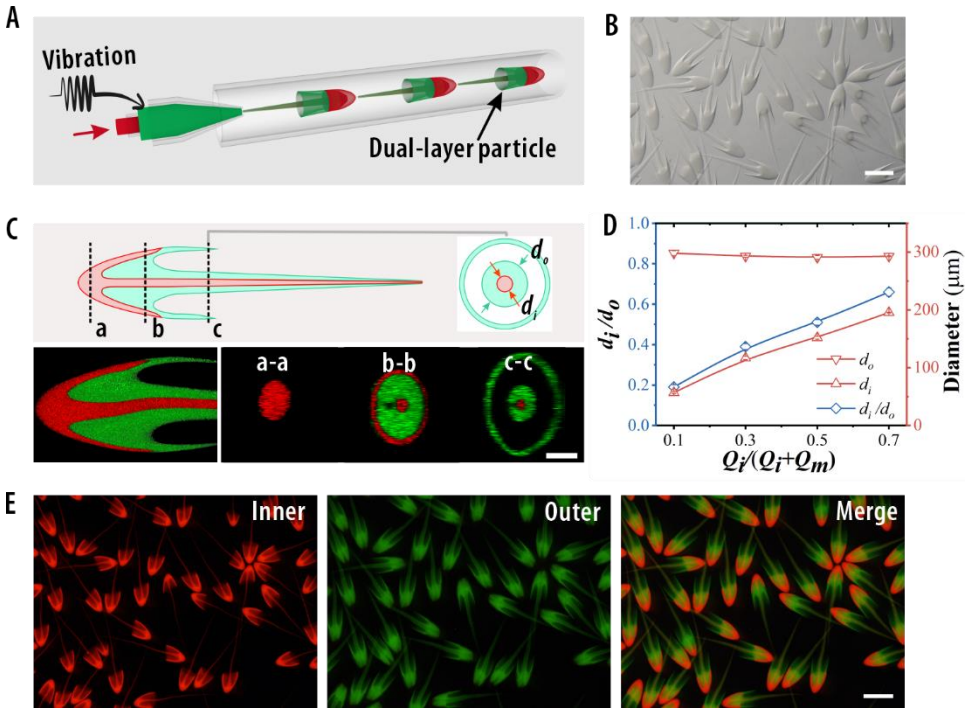

Fig. 4. Formation of the dual-layered jellyfish-like particles in microfluidics. (A) Schematic illustration of the two-stage nested capillary microfluidic device for the generation of dual-layered jellyfish-like microparticles; **(B)** microscopy images of a batch of bio-inspired dual-layered particles; **(C)** schematic illustrations and cross-sectional CLSM images of the resultant particles; **(D)** the ratio of the internal thread diameter d_i to the outer thread diameter d_o as a function of φ; **(E)** fluorescent images of a batch of dual-layered particles with red and green fluorescent polystyrene nanoparticles added to the inner and outer layer, respectively. The scale bars are 1000 μm in (B) and (E), and 200 μm in (C).

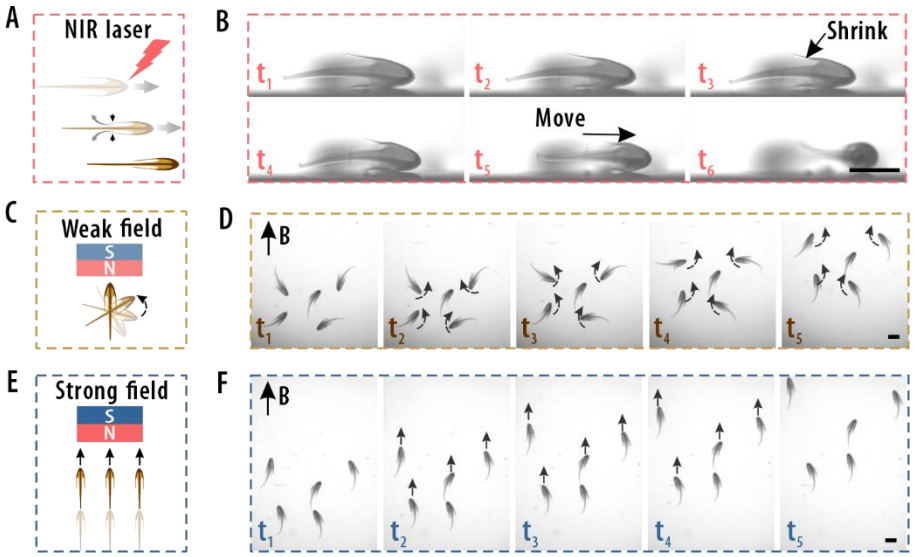

Fig. 5. Stimuli-triggered motion of the dual-layered particles. (A, B) Schematic illustration and real-time images showing the movement of a single dual-layered jellyfish microparticle under NIR laser irradiation; **(C, D)** schematic illustration and real-time images showing the re-orientation of the magnetic-responsive dual-layered jellyfish microparticles under a weak magnetic field; **(E, F)** schematic illustration and real-time images showing the directional migration of the magnetic-responsive dual-layered jellyfish microparticles under a strong magnetic field. The scale bars are 1000 μm.

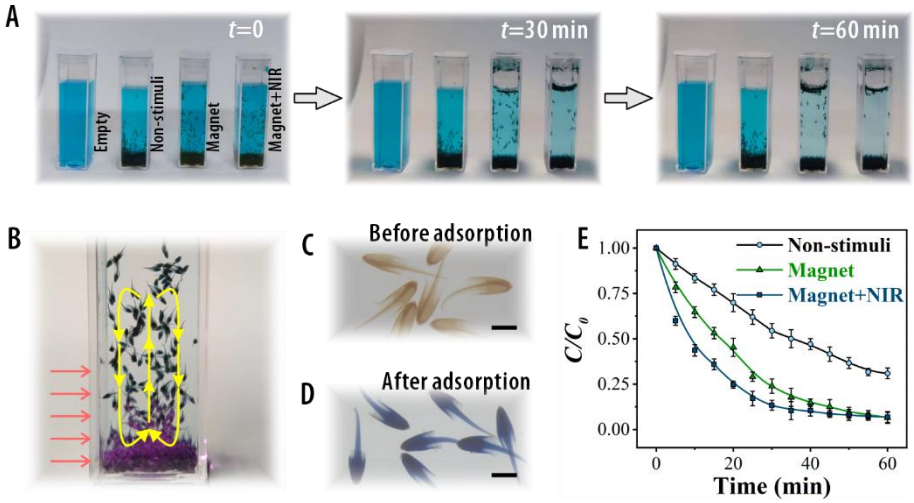

Fig. 6. Adsorption processes of the dual-layer jellyfish particles under different conditions. (A) The adsorption process of MB by using magnetic GO/NIPAM dual-layer jellyfish particles under different stimulation modes; **(B)** the circulation of a swarm of particles under NIR stimulation; **(C, D)** microscopic images of the particles (C) before and (D) after MB adsorption; **(E)** the MB adsorption kinetics of the dual-layer jellyfish particles; C was the real-time concentration and C_0 was the initial concentration of MB. The scale bars are 1000 μm.

481